Matrix isolation infrared spectroscopic and quantum chemical studies on the rotational isomers of orotic acid (6-carboxyuracil)

Rafał Wysokiński [a], Katarzyna Helios [a], Leszek Lapinski [b], Maciej J. Nowak [b], Danuta Michalska [a,*]

[a] Faculty of Chemistry, Wrocław University of Technology, Smoluchowskiego 23, 50-370 Wrocław, Poland
[b] Institute of Physics, Polish Academy of Sciences, Al. Lotników 32/46, 02-668 Warsaw, Poland

ARTICLE INFO

ABSTRACT

The infrared spectrum of orotic acid (6-carboxyuracil) isolated in a low-temperature argon matrix is presented, for the first time. This molecule is a key precursor in the biosynthesis of all pyrimidine nucleotides in living organisms. The comprehensive theoretical studies on the rotational isomerism of orotic acid have been performed by an ab initio MP2 and three density functional methods (B3LYP, M06 and M06-2X). All theoretical methods have predicted that four possible conformers of orotic acid may exist in the gas phase. The calculated barrier height for rotation of the COOH group around the C—C bond (37 kJ mol^{-1}, M06-2X) is much lower than the barriers for the OH rotation around the C—O bond (47 and 51 kJ mol^{-1}). The Gibbs free energies, relative stabilities and the mole fractions of isomers at different temperatures, in the gas phase, have been determined.

The anharmonic vibrational frequencies, infrared intensities and potential energy distributions (PEDs) were computed for two isomers of the lowest energy (A and B) using the B3LYP method with the aug-cc-pVTZ basis set. The theoretical anharmonic IR spectra are in excellent agreement with the experiment. It is concluded that the most stable conformer (A) is the predominant form in a low-temperature argon matrix, while the mole fraction of the less stable B conformer can be assessed as ca. 15%. No spectral indications of the presence of other isomers (C and D) in the matrix were detected.

© 2012 Elsevier B.V. All rights reserved.

1. Introduction

Orotic acid (H$_3$Or, 6-carboxyuracil, also called vitamin B$_{13}$) plays a fundamental role in the biosynthesis of nucleic acids, because it is a key precursor in the pathway to formation of all pyrimidine nucleotides in living organisms [1,2]. Moreover, it is also very important in the metabolism of vitamins B$_6$ (folic acid) and B$_{12}$ (cobalamine). Orotic acid and its metal complexes have attracted much attention in medicine. These compounds display antibacterial and cytostatic properties [3]. Metal-orotates can penetrate the cell membranes; therefore, they can be used in curing syndromes associated with a deficiency of calcium, magnesium, zinc, or iron [4–6]. Both orotic acid and its Mg(II) salt have a beneficial effect in prophylaxis and in treatment of heart and vessels diseases [7–9].

Orotic acid is also an interesting polydentate ligand and its coordination chemistry has been the subject of thorough investigations [10–16]. In a series of papers we have reported the crystal and molecular structures, vibrational spectra and density functional (DFT) studies on Ni(II), Cu(II) and Pt(II) complexes with this ligand

[11–16]. A single crystal X-ray analysis of orotic acid monohydrate was published by Takusagawa and Shimada [17] and also by Portalone [18]. Hernanz et al. [19] studied the IR and Raman spectra of polycrystalline orotic acid and its deuterated isotopomers.

Rotational isomerism is an intriguing feature of carboxylic acids [20]. Therefore, we have performed thorough quantum chemical studies on this phenomenon, in orotic acid. The barrier heights for the internal rotations of the COOH and OH groups, the Gibbs free energies, and the relative stabilities of the conformers in the gas phase have been calculated by means of an ab initio MP2 and density functional theory methods.

In the literature, there are numerous papers devoted to matrix isolation vibrational spectroscopy of uracil and its derivatives, however, 6-carboxyuracil (orotic acid) has not been studied as yet. In view of the biological significance of this molecule, a full understanding of its vibrational spectrum is of great importance. In this work, the FT-IR spectrum of orotic acid monomers isolated in a low temperature argon matrix is reported for the first time. The anharmonic frequencies have been calculated for the two most stable conformers of the title molecule using the B3LYP method with the aug-cc-pVTZ basis set. On the basis of the combined experimental and theoretical investigations, the presence of different isomers of orotic acid in the solid argon is discussed.

* Corresponding author. Tel.: +48 71 3203759; fax: +48 71 3204360.
E-mail address: danuta.michalska@pwr.wroc.pl (D. Michalska).

2. Experimental

Anhydrous orotic acid (purity >98%) was purchased from Aldrich Chemical Co. The sample of the solid compound was electrically heated in a miniature glass oven placed in the vacuum chamber of a continuous-flow helium cryostat. The temperature of evaporation of orotic acid was ca. 480 K. The argon matrix gas of spectral purity (6.0) was supplied by Linde AG. The method of matrix preparation and the apparatus were the same as described elsewhere [21]. The vapors of the compound were deposited together with a large excess of inert gas (argon) on a CsI window cooled to 10 K. The IR spectra were recorded with 0.5 cm^{-1} resolution using a Thermo Nicolet Nexus 670 FTIR spectrometer equipped with a KBr beam splitter and a DTGS detector. Intensities of the IR absorption bands were measured by numerical integration.

3. Computational

The optimized geometries and harmonic frequencies of the four possible isomers of orotic acid, and the energies of the rotational barriers were calculated at different levels of theory. We have used the well known B3LYP method [22,23] and two new hybrid meta exchange-correlation functionals developed by Zhao and Truhlar [24], called M06 and M06-2X. The M06 functional is parametrized including both transition metals and nonmetals, whereas M06-2X is parametrized only for nonmetals (2X means double the amount of nonlocal exchange). The two latter functionals are highly recommended for theoretical study of thermochemistry, kinetics and reaction barriers [24,25]. In all DFT calculations the aug-cc-pVTZ basis set [26,27] has been used. This is the correlation-consistent, polarized valence triple-zeta basis set augmented with diffuse functions on all atoms. An ab initio second order perturbation Møller–Plesset method, all-electron MP2 [28], was combined with two basis sets, aug-cc-pVTZ and D95V(d,p) [29].

The potential energy curve for the rotation of the COOH group was computed as a relaxed potential energy surface (PES) scan [30]. The optimized structure of conformer A (see Fig. 1) was used as the starting geometry and the carboxylic group was systematically rotated around the exocyclic C6—C7 bond by varying the O8=C7—C6—N1 torsional angle in 10° increments. At each step, all the remaining geometry parameters were reoptimized. Since both conformers A and B are planar, the relaxed scan procedure was performed in the range 0–180°. The analogous relaxed PES scans have been performed for rotation of the O—H bond around the C—O bond, by varying the H14—O9—C7—C6 torsional angle in A and B conformers. The harmonic vibrational frequencies calculated for the minima on the PES indicate that the corresponding structures are stable (all frequencies are real).

In optimization of the transition state for the internal rotation we have used a synchronous transit-guided quasi-Newton (STQN) method [31] implemented to the Gaussian programs (QST3 option). The first-order saddle point (transition state) was confirmed by the calculations of vibrational frequencies at each level of theory (one imaginary frequency was obtained). The barrier height for the rotation of the COOH or OH groups was defined as the difference between the energy of the transition state and the lowest energy equilibrium structure.

To determine the relative stability of all conformers of orotic acid, the Gibbs free energies ($G°_T$) have been calculated (independently) for the temperatures $T = 400$ and 480 K by means of the B3LYP, M06 and MP2 methods.

For the two conformers of the lowest energy (A and B) the anharmonic vibrational frequencies (and harmonic infrared intensities) were calculated at the B3LYP/aug-cc-pVTZ level. In anharmonic computations the algorithm elaborated by Barone [32,33] has been

used. This is a second-order perturbative treatment (PT) based on quadratic, cubic, and semi-diagonal quartic force constants. The calculations were performed with the Gaussian 09 set of programs [34].

To provide detailed vibrational assignments of the experimental spectra, normal coordinated analysis has been carried out [21]. A non-redundant set of 39 symmetrized internal coordinates has been defined (see Supplementary material). The DFT-calculated force constants were transformed from Cartesian coordinates to internal coordinates and the potential energy distribution (PED) matrices were calculated as described previously [35,36]. The simulated infrared spectra were plotted using a Lorentzian band shape with a half-width at half-maximum (HWHM) of 1 cm^{-1} (the intensities at the simulated maxima are equal to the calculated IR intensities).

4. Results and discussion

4.1. Relative stabilities, barriers to the COOH and OH internal rotations and geometries of the conformers

Fig. 1 illustrates the optimized structures of four possible isomers of orotic acid, denoted as A, B, C and D, which, hypothetically, can be present in the gas phase. In A, the carboxylic C7=O8 bond is in the *trans* position with respect to the C5=C6 double bond of the uracil ring, while in B, the C7=O8 bond is in *cis* orientation with respect to C5=C6. In both A and B conformers the O—H group eclipses the carboxylic C7=O8 bond (this is the *syn* or the *Z* form of carboxylic acids [20]). Isomers C and D have been derived from A and B, respectively, by rotation of the O9—H14 bond around the C7—O9 bond. In both C and D, the OH group has an *anti* conformation with respect to the C7=O8 bond (the E form [20]).

According to the calculations, only the A and B conformers are definitely planar. As is seen in Fig. 1, in the case of isomer C, the C7=O8 group is oriented toward the N1—H15 group of the uracil ring, which allows a weak electrostatic interaction between the O8 and H15 atoms. By contrast, in isomer D, a repulsion between the H14 and H15 atoms leads to a significant distortion from planarity, and makes this structure the least stable. In isomer C, the O8C7C6N1 dihedral angle ($\varphi 1$) varies in the range from 1.1° (B3LYP) to 14.0° (MP2). In isomer D, the carboxyl group is tilted by about 30–32°, out of the plane of the uracil ring. The values of selected dihedral angles are listed in Supplementary material.

Table 1 lists the calculated energies of the four conformers. All the density functional methods indicate that B, C and D are less stable than conformer A, by about 7, 23 and 44 kJ mol^{-1}, respectively. Calculations performed at the MP2/D95V(d,p) level yield a slightly smaller energy difference between conformers A and B

Table 1
The relative energies (in kJ mol^{-1}) of conformers A, B, C and D and the barrier heights (kJ mol^{-1}) for rotation of the COOH and OH groups in orotic acid calculated by the density functional (B3LYP, M06, M06-2X) and ab initio MP2 methods.

Energy	B3LYP/I	M06/I	M06-2X/I	MP2/II
A	0[a]	0[b]	0[c]	0[d]
B	6.96	7.30	7.35	5.14
C	22.76	21.90	22.76	28.74
D	44.11	44.12	44.33	47.04
Barrier height				
A → B	33.90	37.49	37.10	34.69
A → C	49.10	50.19	47.46	53.46
B → D	52.52	53.84	51.28	57.12

The following basis sets have been used: aug-cc-pVTZ, denoted as I and D95V(d,p) denoted as II.
For the most stable conformer A, the absolute energy values $E°$ (in hartrees):
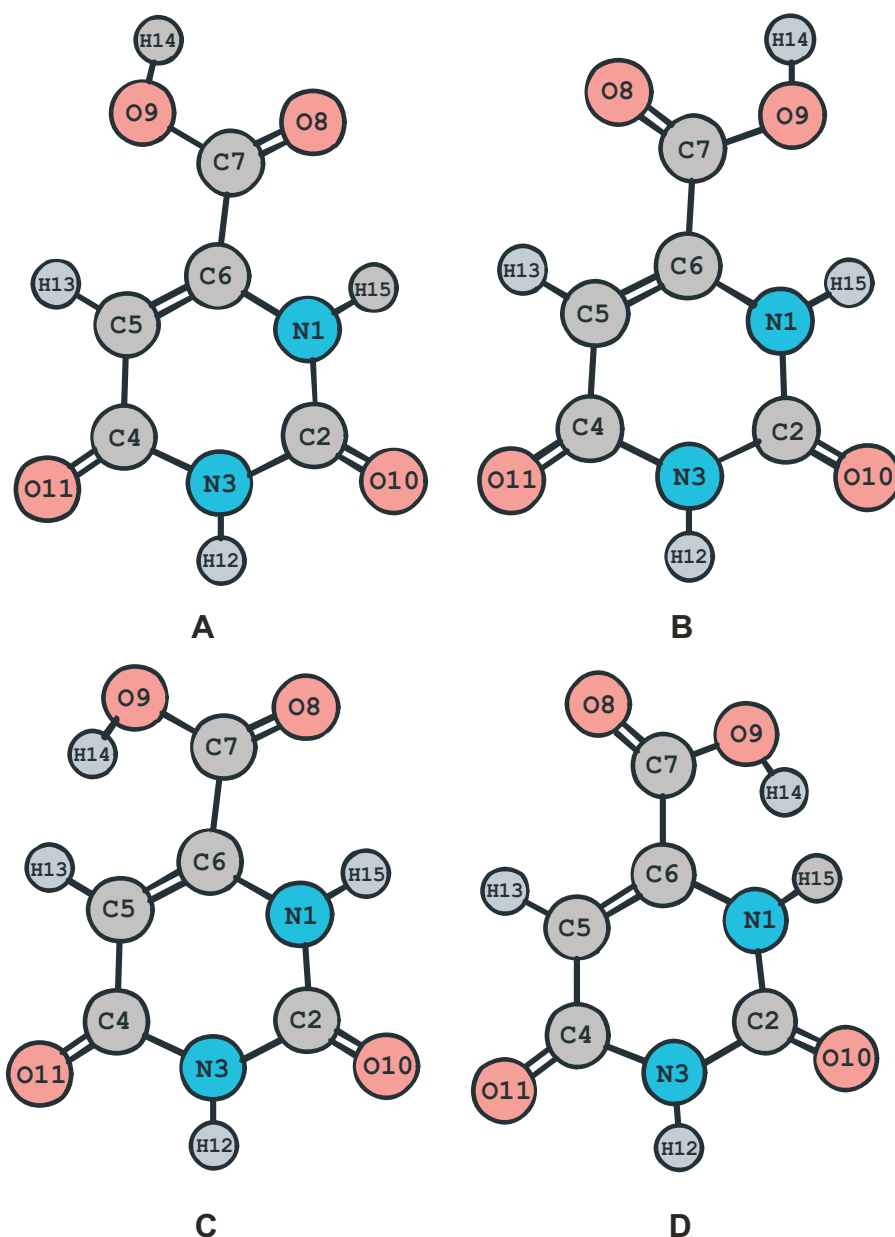[a] 603.6343168; [b] 603.2846002; [c] 603.4172736; [d] 601.860168.

Fig. 1. Diagram showing the four optimized structures of orotic acid conformers and the numbering of atoms.

($5.1 \, kJ \, mol^{-1}$). In the theoretical studies on 2-hydroxybenzoic acid, the energy differences between the two most stable conformers, calculated at the MP2/6-311 + G(d,p) level of theory, was found to be $11.7 \, kJ \, mol^{-1}$ (one of the conformers was stabilized by intramolecular O—H⋯O hydrogen bond) [37].

To explore the A → B conversion in orotic acid, the barrier height for the rotation of the COOH group around the C6—C7 bond has been studied. Fig. 2 illustrates the shape of the potential energy for the COOH rotation (red triangles) computed from a relaxed potential energy surface (PES) scan at the M06/aug-cc-pVTZ level (very similar scan has been obtained by the B3LYP method, see Supplementary material). In the transition state (TS) the orientation of the carboxylic group is nearly perpendicular to the plane of the uracil ring.

The accurate energies of the transition states for the internal rotations have been calculated by a synchronous transit-guided quasi-Newton (STQN) method [31]. Table 1 lists the energy barriers

for the rotation of the COOH group determined at various levels of theory. All the DFT methods consistently indicate that the barrier height for the rotation of the COOH group around the C6—C7 bond is about five times larger than the energy difference between B and A.

Very recently, an assessment of the performance of a wide range of functionals for calculations of thermochemistry, kinetics and reaction barriers has been reported [25]. Among the 27 tested density functional methods (including GGA, hybrid and range-separated functionals), the M06-2X method was shown to be the best for predicting the barrier heights. Therefore, it seems that the barrier height for the internal rotation of the carboxylic COOH group in orotic acid, $37.1 \, kJ \, mol^{-1}$, calculated at the M06-2X/aug-cc-pVTZ level, is reliable.

As follows from the results collected in Table 1, the barrier for rotation of the hydroxyl O—H bond around the C7—O9 bond is much larger than that for rotation of the COOH group around the C6—C7
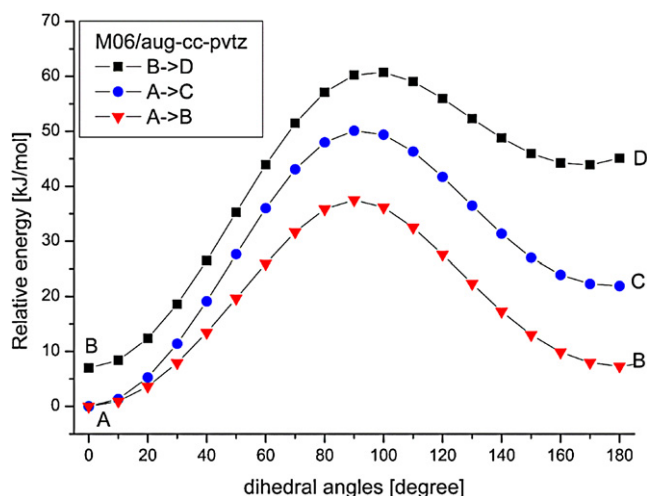
Fig. 2. Relaxed potential energy surface (PES) scan of the rotation of the COOH group around the C6—C7 bond (A → B, red triangles), relaxed PES scan of the rotation of the O—H bond in A around the C7—O9 bond (A → C, blue circles) and relaxed PES scan of the rotation of the O—H bond in B around the C7—O9 bond (B → D, black squares). Calculations performed by the M06 method with the aug-cc-pVTZ basis set. (For interpretation of the references to color in figure legend and text, the reader is referred to the web version of the article.)

bond. The barrier heights are 47.5 and 51.3 kJ mol^{-1} for the O—H rotation in conformers A and B, respectively (the M06-2X calculations). The relaxed PES scans for the OH rotation in two conformers are illustrated in Fig. 2.

A reliable estimation of the relative stability and the mole percentages of all isomers in the gas phase can be obtained from the calculated Gibbs free energies (ΔG°_T), similarly as it has been done for cytosine tautomers [38]. In the calculations of the equilibrium Boltzmann populations the degeneracy of the lower symmetry conformers has been taken into account. In orotic acid only the conformers A and B are strictly planar (see Supplementary material), therefore the degeneracies of these isomers are equal to 1. In the case of the nonplanar isomers C and D (which belong to the C_1 symmetry point group) the degeneracies were assumed to be equal to 2.

Table 2 lists the relative ΔG°_T calculated for $T = 400$ K and $T = 480$ K by using the B3LYP, M06 and MP2 methods ($T = 480$ K is the temperature of evaporation of orotic acid). As is seen in Table 2, all the theoretical methods consistently predict a decrease of ΔG°_T for conformer B with an increase of the temperature of the gas phase. This is accompanied by an increase of the calculated mole fraction of B. According to the results obtained by the B3LYP method the population of A, B, C and D isomers should be equal to 76.8%, 17.6%, 5.6% and 0.0%, respectively (480 K). The M06 functional predicts a somewhat higher population of conformer B (19.9%) while an ab initio MP2 method gives the highest mole fraction of B (25.9%) for

$T = 480$ K. As will be shown later, the mole fraction of B, obtained experimentally from the matrix isolation infrared spectra, is in quite good agreement with the B3LYP results.

Table 3 lists the bond lengths and bond angles of conformers A and B computed by the MP2, M06 and B3LYP methods using the aug-cc-pVTZ basis set. The experimental X-ray data determined for conformer A [18] are also included in this table, for comparison. The corresponding geometrical parameters calculated by the three theoretical methods are similar and they show good overall agreement with the experiment. In particular, the single C—N and C—C bond lengths computed by the MP2 and M06 methods are very similar. However, the M06 method gives the C5=C6 double bond length (1.340 Å) too short, by 0.12 Å, in comparison to the experiment. Of the two exocyclic carbonyl groups, the C2=O10 atom distance is shorter, by about 0.006 Å, than the C4=O11 bond length (in the crystal this difference is bigger due to the intermolecular hydrogen bond involving the C4=O11 carbonyl group).

In conformer A, the C7=O8 group is oriented toward the N1—H15 group. This orientation leads to a weak electrostatic interaction between O8 and H15 atoms, which may elongate the carboxylic C=O bond. Indeed, the theoretical calculations consistently predict that the C7=O8 inter-atomic distance in conformer A is longer, by 0.006 Å, than that in B. On the other hand, the calculated carboxylic C7—O9 bond length in A is shorter, by about 0.012 Å, than that in B. The experimentally determined bond lengths of the carboxylic group of orotic acid monohydrate are strongly affected by intermolecular hydrogen bonds with water molecule, in the crystal [17,18].

A main structural difference between A and B is the tilt of the C6—C7 bond toward the N1 atom, in conformer A. According to the X-ray data, the C5—C6—C7 angle (124.0°) is larger, by about 10°, than the N1—C6—C7 angle (113.8°). The theoretical methods predicted both these bond angles in very good agreement with experiment. It should be noted that in conformer B, the calculated C5—C6—C7 angle is smaller than that in A by about 4°, and consequently, the N1—C6—C7 angle is larger, in comparison to A (Table 3).

4.2. The infrared spectra of orotic acid monomers

The harmonic and anharmonic vibrational frequencies, infrared intensities and potential energy distributions (PEDs) have been computed at the B3LYP/aug-cc-pVTZ level for conformers A and B (the results are collected in Table 4). Figs. 3–5 compare the IR spectrum of orotic acid monomers isolated in a low-temperature argon matrix with the theoretical spectra. The comparison has shown that the calculated anharmonic IR spectrum for conformer A matches the experimental spectrum very well (some bands due to B conformer have also been identified in the regions 3700–3000 and 1900–1600 cm^{-1}). The bands observed in the experimental IR spectrum along with their assignments are collected in Table 5.

Table 2
The relative Gibbs free energies (ΔG°_T, kJ mol^{-1}) and the mole fractions (percentages) of conformers A, B, C and D of orotic acid ($T = 400$ and 480 K).

Form	Degen.	B3LYP/aug-cc-pVTZ				M06/aug-cc-pVTZ				MP2/D95V(d,p)			
		ΔG_{400} [a]	%	ΔG_{480} [b]	%	ΔG_{400} [c]	%	ΔG_{480} [d]	%	ΔG_{400} [e]	%	ΔG_{480} [f]	%
A	1	0.00	83.9	0.00	76.8	0.00	84.0	0.00	78.3	0.00	78.3	0.00	73.5
B	1	6.02	13.7	5.87	17.6	5.65	15.4	5.45	19.9	4.27	21.7	4.17	25.9
C	2	14.18	2.4	13.21	5.6	18.58	0.6	17.93	1.8	26.74	0.00	22.28	0.6
D	2	41.30	0.0	41.93	0.0	41.97	0.0	41.69	0.0	45.23	0.00	45.01	0.0

Abbreviations: Degen. = degeneracies for different forms (conformers). For the most stable conformer A, the Gibbs free energy values in hartrees: [a] $G^{\circ}_{400} = -603.583679$; [b] $G^{\circ}_{480} = -603.597685$; [c] $G^{\circ}_{400} = -603.233444$; [d] $G^{\circ}_{480} = -603.247451$; [e] $G^{\circ}_{400} = -601.808766$; [f] $G^{\circ}_{480} = -601.822865$. The G°_T values were calculated independently at each temperature (400 and 480 K).

Table 3
Selected geometrical parameters of orotic acid (conformers A and B), calculated by ab initio MP2 and two DFT methods (M06 and B3LYP) using the aug-cc-pVTZ basis set (I).

Parameter[a]	Exp.[b]	MP2/I		M06/I		B3LYP/I	
		A	B	A	B	A	B
N1—C6	1.366	1.368	1.371	1.366	1.370	1.371	1.375
N1—C2	1.370	1.382	1.384	1.381	1.383	1.385	1.387
C2—N3	1.377	1.384	1.382	1.381	1.379	1.385	1.383
N3—C4	1.372	1.398	1.400	1.398	1.399	1.401	1.403
C4—C5	1.439	1.455	1.454	1.455	1.454	1.460	1.458
C5—C6	1.352	1.353	1.353	1.340	1.339	1.347	1.346
C6—C7	1.501	1.487	1.490	1.487	1.489	1.494	1.496
C2—O10	1.224	1.215	1.216	1.201	1.202	1.210	1.210
C4—O11	1.242	1.221	1.221	1.205	1.205	1.214	1.213
C7—O8	1.206	1.213	1.207	1.199	1.193	1.206	1.200
C7—O9	1.304	1.341	1.353	1.330	1.342	1.340	1.353
O9—H14	0.89	0.971	0.971	0.966	0.966	0.969	0.969
N1—H15	0.85	1.012	1.009	1.010	1.007	1.010	1.007
C6—N1—C2	122.4	123.5	123.4	123.6	123.5	123.7	123.5
N1—C2—N3	114.8	112.8	113.0	112.8	112.9	113.1	113.2
C2—N3—C4	126.3	128.5	128.5	128.4	128.3	127.9	127.9
N3—C4—C5	115.7	113.6	113.5	113.4	113.4	113.7	113.7
C4—C5—C6	118.6	119.3	119.6	119.6	119.9	119.6	119.9
C5—C6—C7	124.0	124.5	120.3	124.5	120.1	124.6	120.5
N1—C6—C7	113.8	113.2	117.6	113.3	117.9	113.4	117.8
C6—C7—O8	120.3	122.6	124.7	122.5	124.5	122.5	124.6
C6—C7—O9	114.0	112.8	111.1	112.9	111.4	113.2	111.5
O8—C7—O9	125.7	124.7	124.2	124.6	124.1	124.3	123.8
C6—N1—C2—N3	2.20	0.0	0.0	0.0	0.0	0.0	0.0
O8—C7—C6—N1	−1.87	0.0	180.0	0.0	180.0	0.0	180.0
O9—C7—C6—N1	178.2	180.0	0.0	180.0	0.0	180.0	0.0

[a] The atom numbering is shown in Fig. 1.
[b] Experimental data are from an X-ray crystal structure of orotic acid monohydrate (conformer A is present in the crystal) [18].

4.2.1. O—H, N—H and C—H stretching modes

The 3700–3200 cm^{-1} region of the experimental and theoretical IR spectra of orotic acid is shown in Fig. 3a. Two intense bands, at 3563 cm^{-1} and 3428 cm^{-1}, dominate this range of the experimental IR spectrum. The higher wavenumber band undoubtedly arises from the stretching vibration of the OH bond in the carboxylic COOH group. The predicted anharmonic frequencies of the ν(O—H) vibrations in conformers A (3555 cm^{-1}) and B (3550 cm^{-1}) are very similar to one another (Table 4). Hence, if B is populated in a low-temperature Ar matrix, its ν(O—H) band would only contribute to a broadening of the experimental band at 3563 cm^{-1}, which is attributed mainly to A. The wavenumber of the ν(O—H) band observed for orotic acid, is very similar to that of the analogous ν(O—H) band, which was found at 3567 cm^{-1} in the spectrum of benzoic acid monomers isolated in solid argon [39].

Population of isomers C or D in the matrix would manifest itself by appearance of the ν(O—H) bands at a higher wavenumber region than those of the ν(O—H) bands in the spectra of A or B. The calculated harmonic frequencies of the ν(O—H) vibrations in C and D are 3789 and 3764 cm^{-1}, respectively. Using a scaling factor of 0.952 (derived from the $\nu^{\text{anh}}/\nu^{\text{harm}}$ ratio of anharmonic and harmonic frequencies calculated for the OH stretching mode in A), the estimated anharmonic ν(O—H) frequencies in C and D should be 3607 and 3583 cm^{-1}, respectively. An examination of the experimental spectrum shows no visible bands at these wavenumbers.

In the 3500–3400 cm^{-1} range, two bands (an intense one at 3428 and a much weaker band at 3460 cm^{-1}) appear in the experimental spectrum of orotic acid. These bands should be assigned to the stretching vibrations of the N—H bonds. In the theoretical spectrum of the most stable conformer (A), two closely spaced IR bands are predicted with the anharmonic frequencies 3423 and 3419 cm^{-1}. Both the frequencies are quite close to the spectral position of the intense band observed in the experimental spectrum at 3428 cm^{-1}. Hence, most probably, the two bands overlap and contribute to the high intensity of this experimental

band. According to the PED calculated for A, the corresponding two normal modes (2A and 3A) can be described as strongly coupled ν(N3—H) and ν(N1—H) stretching vibrations (Table 4).

The calculation performed for conformer B predicts two bands, at 3464 and 3427 cm^{-1}, which are due to the ν(N1—H) and ν(N3—H) stretching vibrations, respectively. The calculated anharmonic frequency of the ν(N1—H) mode is in very good agreement with the position of a weak experimental band observed at 3460 cm^{-1}. Therefore, this band is most probably a spectral signature of the presence of B, in the matrix. The low intensity of the band at 3460 cm^{-1} indicates that the amount of matrix-isolated B must be relatively small. The calculated frequency of the ν(N3—H) mode in B (3427 cm^{-1}) suggests that the corresponding band is probably hidden under the strong experimental band at 3428 cm^{-1}, which is attributed mainly to A (see Table 5).

The C—H stretching modes usually generate bands of very low intensity in the IR spectra of matrix-isolated monomeric heterocycles. However, these modes are quite strong in the Raman spectra of such molecules [35,36,40–46]. In the Raman spectrum of crystalline orotic acid, a distinct band at 3098 cm^{-1} has been assigned to the ν(C5—H) stretching vibration [19] which is supported by our calculated anharmonic frequency, 3118 cm^{-1}.

4.2.2. C=O and C=C stretching modes

In the 1900–1600 cm^{-1} range of the experimental spectrum of orotic acid isolated in an Ar matrix (see Fig. 3b) a complicated pattern of infrared bands is observed. Similar complicated IR spectra in this range have been reported for matrix-isolated uracil, thymine and their derivatives [36,40–46]. This effect has been attributed to multiple Fermi resonances between the ν(C=O) fundamentals and various combination transitions or overtones.

The strong experimental band at 1761 cm^{-1} should be assigned to the ν(C2=O) stretching vibrations in both conformers. The calculated anharmonic frequencies of the ν(C2=O) modes in A and B are 1759 and 1762 cm^{-1}, respectively. These theoretical values are

Table 4

Theoretical anharmonic frequencies (ω^{an}, cm^{-1}), harmonic frequencies (ω^{har}, cm^{-1}) and infrared intensities (A, km mol^{-1}) calculated for two conformers (A and B) using the B3LYP method with the aug-cc-pVTZ basis set.

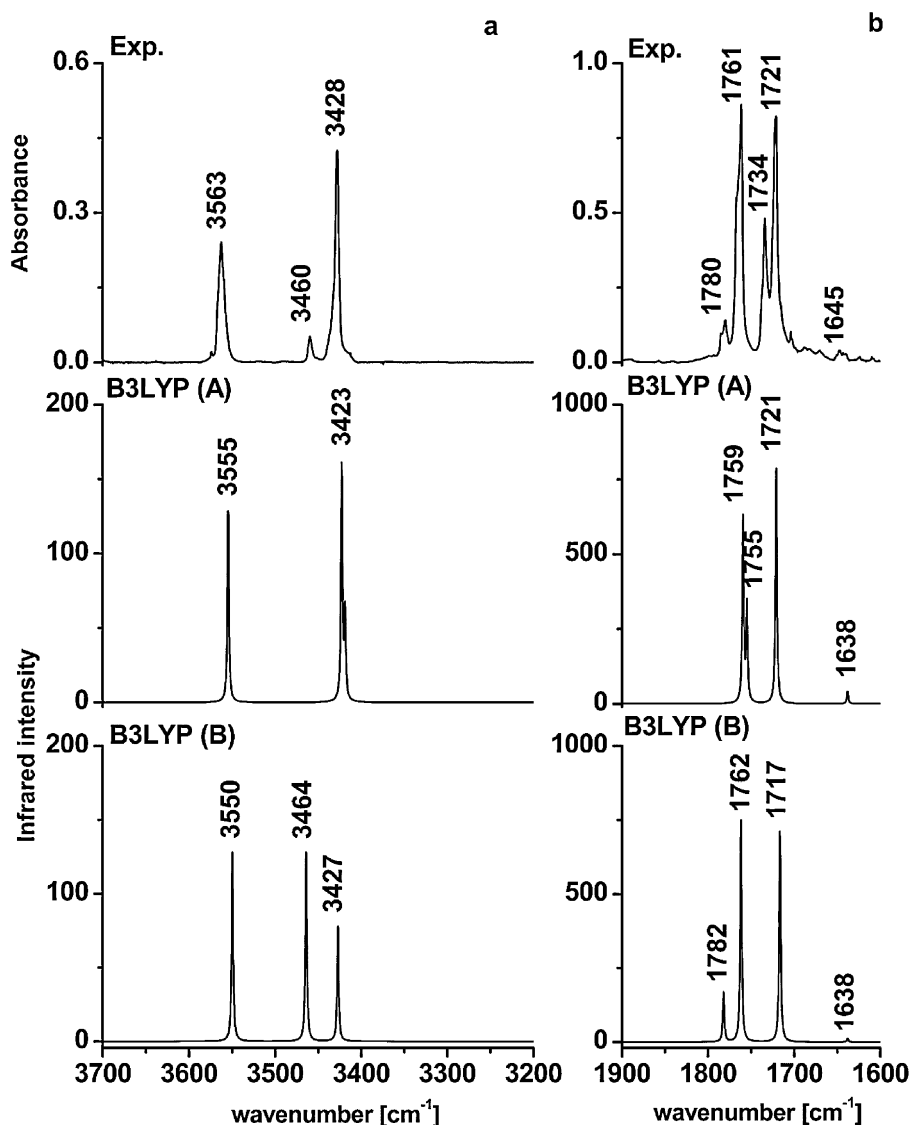| Conformer A					Conformer B				
Mode no.	ω^{an}	ω^{har}	A	PED (%)[a]	Mode no.	ω^{an}	ω^{har}	A	PED (%)[a]
1A	3555	3743	129	νOH (100)	1B	3550	3745	128	νOH (100)
2A	3423	3588	158	νN3H (+70), νN1H (−30)	2B	3464	3623	128	νN1H (100)
3A	3419	3589	58	νN1H (+70), νN3H (+30)	3B	3427	3588	78	νN3H (100)
4A	3118	3259	8	νC5H (100)	4B	3118	3251	10	νC5H (100)
5A	1759	1797	616	νC2=O (89)	5B	1782	1816	167	νC7=O8 (85)
6A	1755	1789	323	νC7=O8 (87)	6B	1762	1795	749	νC2=O (89)
7A	1721	1758	786	νC4=O (89)	7B	1717	1761	711	νC4=O (89)
8A	1638	1671	41	νC5=C6 (79)	8B	1638	1673	12	νC5=C6 (80)
9A	1487	1522	91	νU$_{ring}$ (50), δN1H (26)	9B	1470	1511	151	νU$_{ring}$ (44), δN1H (31)
10A	1364	1408	39	δN3H (61), νU$_{ring}$ (17)	10B	1359	1407	16	δN3H (58), νU$_{ring}$ (19)
11A	1373	1395	134	νU$_{ring}$ (79), δN1H (10)	11B	1366	1399	96	νU$_{ring}$ (58), δN1H (12)
12A	1346	1387	147	δOH (27), νC7O9 (23), νU$_{ring}$ (10)	12B	1324	1365	200	νU$_{ring}$ (37), δOH (27), νC7O9 (14)
13A	1294	1322	9	δC5H (41), δN1H (36), δOH (10)	13B	1282	1313	4	δC5H (43), δN1H (21), δOH (24)
14A	1169	1217	19	νU$_{ring}$ (62), δC5H (17)	14B	1175	1213	74	νU$_{ring}$ (72), δC5H (15)
15A	1134	1177	318	δOH (42), νC7O9 (28), νC6C7 (11)	15B	1124	1164	332	δOH (42), νC7O9 (21), νC6C7 (12)
16A	1096	1120	25	νU$_{ring}$ (51), δC5H (24), δN1H (15)	16B	1074	1100	22	νU$_{ring}$ (34), δC5H (22), νC7O9 (21)
17A	1006	1024	14	δ(R1)$_U$ (69)	17B	1003	1020	41	δ(R1)$_U$ (62)
18A	978	1000	10	νU$_{ring}$ (70), δ N3H (12)	18B	978	1001	17	νU$_{ring}$ (72), δ N3H (10)
19A	896	913	13	νU$_{ring}$ (74)	19B	892	910	7	νU$_{ring}$ (84)
20A	870	888	17	γC5H (84), γC4=O (14)	20B	882	898	20	γC5H (60), τU$_{ring}$ (18), γC6C7 (12)
21A	789	802	56	γCOO (74), γC4=O (16)	21B	787	794	56	γCOO (79), γC4=O (14)
22A	763	771	49	γC2=O (78), γN3H (17)	22B	764	771	48	γC2=O (75), γN3H (19)
23A	730	742	11	γC4=O (39), τU$_{ring}$ (28), γC2=O (22)	23B	733	743	9	γC4=O (44), τU$_{ring}$ (26), γC2=O (22)
24A	680	691	50	δ_{sc}COO (67), δU$_{ring}$ (15)	24B	671	689	41	δ_{sc}COO (67), δU$_{ring}$ (15)
25A	678	685	57	γN3H (77), τU$_{ring}$ (23)	25B	675	681	51	γN3H (76), τU$_{ring}$ (23)
26A	627	632	4	δC2=O (26), δC4=O (24), ρCOO (14)	26B	622	624	2	δC2=O (29), δC4=O (27), ρCOO (16)
27A	631	631	32	γN1H (85)	27B	608	621	51	τOH (61), γN1H (13)
28A	594	608	117	τOH (89)	28B	592	585	110	γN1H (78), τOH (21),
29A	565	572	<1	δU$_{ring}$ (63), δ_{sc}COO (13)	29B	568	574	8	δU$_{ring}$ (70), δ_{sc}COO (13)
30A	525	530	21	δ(R3)$_U$ (74)	30B	526	532	19	δ(R3)$_U$ (75)
31A	475	481	4	γCOO (61), τU$_{ring}$ (31)	31B	487	477	3	γCOO (60), τU$_{ring}$ (36)
32A	424	430	2	ρCOO (49), δU$_{ring}$ (20), δC2=O (12)	32B	424	428	4	ρCOO (51), δU$_{ring}$ (23) δC4=O (10)
33A	405	407	38	δU$_{ring}$ (38), δC2=O (27), δC2=O (16)	33B	407	407	33	δU$_{ring}$ (51), δC2=O (21), δC4=O (19)
34A	333	337	1	δU$_{ring}$ (51), δ_{sc}COO (14)	34B	333	338	1	δU$_{ring}$ (55), δ_{sc}COO (14), δC4=O (13)
35A	174	176	4	δC6C7 (65), ρCOO (22)	35B	183	178	2	δC6C7 (66), ρCOO (20)
36A	182	181	<1	τU$_{ring}$ (85), τCOO (14)	36B	187	181	<1	τU$_{ring}$ (87), τCOO (13)
37A	161	159	2	τU$_{ring}$ (100)	37B	159	156	3	τU$_{ring}$ (100)
38A	131	124	2	τU$_{ring}$ (65), γC6C7 (30)	38B	137	125	2	τU$_{ring}$ (69), γC6C7 (29)
39A	70	66	1	τCOO (89), τU$_{ring}$ (10)	39B	51	57	1	τCOO (90), τU$_{ring}$ (10)

[a] *Abbreviations*: ν, stretching; δ, in-plane bending; δ_{sc}, scissoring; ρ, rocking; γ, out-of-plane bending; τ, torsion. The column shows the predominant components of the PED matrix or the sum of internal coordinates (in the case of strongly mixed coordinates of the uracil ring). For example, the sum of individual contributions from the stretching coordinates of the ring is described as νU$_{ring}$. Similarly, δU$_{ring}$ denotes the sum of the in-plane bending coordinates, while τU$_{ring}$ denotes the sum of the torsion coordinates. For the description of δ(R1)$_U$ and δ(R3)$_U$ and other internal coordinates see Table 1S in Supplementary materials.

very close to the spectral position of the experimental band. The configuration of the carboxylic group does not significantly affect the C2=O fragment of the molecule. Therefore, the frequencies of the ν(C2=O) stretching vibrations are so similar in both conformers.

On the other hand, the conformational change from A to B (or vice versa) should significantly affect the C7=O8 double bond in the carboxylic group. In A, the C7=O8 fragment is involved in an interaction with the N1—H15 group, whereas in B such interaction is absent. In the case of A, the electrostatic attraction between the O8 and H15 atoms can lead to an elongation of the C7=O8 (as well as N1—H15) bonds. This is accompanied by a lowering of the frequency of the stretching vibrations of these bonds. Indeed, the calculated anharmonic frequencies of the ν(C7=O8) stretching vibrations in A and B are quite different: 1755 and 1782 cm^{-1}, respectively (see Table 4). Thus, in conformer A both the ν(C7=O8) and ν(C2=O) modes contribute to the experimental IR absorption at 1761 cm^{-1}. For B, the experimental counterpart of the theoretical ν(C7=O8) stretching mode is probably the relatively weak band observed at 1780 cm^{-1} (see Fig. 3b and Table 5). This band can be treated as another (alongside the feature at 3460 cm^{-1}) spectral indication of B conformer trapped in an Ar matrix. However,

one should be very cautious using the experimental intensity of the band at 1780 cm^{-1} (with a shoulder at 1785 cm^{-1}) as a measure of the relative amount of B in the matrix. In the IR spectra of uracil, thymine, and their methyl derivatives, the region corresponding to the ν(C=O) stretching vibrations is full of multiply split bands and some of such components (combination bands) can also contribute to the intensity of the band assigned to ν(C7=O8) in B.

The calculated anharmonic frequencies of the ν(C4=O) stretching vibrations in conformers A and B are very similar to each other (1721 and 1717 cm^{-1}, respectively) and are significantly lower than those of the ν(C2=O) and ν(C7=O8) modes. Hence, both the ν(C4=O) stretching vibrations in A and B should be assigned to a strong experimental band observed at 1721 cm^{-1} (see Fig. 3b). The distinct band observed in the experimental spectrum at 1734 cm^{-1} is probably a result of Fermi-resonance between the combination (1212 + 523) and ν(C=O) fundamental transition. In the IR spectrum of uracil isolated in a low temperature argon matrix, similar split bands at 1741 and 1733 cm^{-1} were assigned to the combination transitions involving the stretching and bending vibrations of the uracil ring [40].

Fig. 3. Comparison of the experimental IR spectra of orotic acid isolated in an argon matrix with the theoretical spectra calculated for conformers A and B at the B3LYP/aug-cc-pVTZ level. (a) Region 3700–3200 cm^{-1} and (b) region 1900–1600 cm^{-1}. The theoretical wavenumbers were computed using the anharmonic approach and the IR intensities were calculated within the harmonic approximation.

The calculated anharmonic frequency of the ν(C5=C6) stretching vibration, 1638 cm^{-1}, is the same for both conformers. The corresponding experimental IR band at 1645 cm^{-1}, in the spectrum of matrix-isolated orotic acid, is extremely weak. However, in the Raman spectrum of crystalline orotic acid [19] a shoulder at 1644 cm^{-1} confirms this assignment.

4.2.3. Other modes

The comparison of the experimental IR spectrum of orotic acid with the theoretical spectra of conformers A and B, in the 1600–800 cm^{-1} range, is shown in Fig. 4. The split band with a maximum at 1392 cm^{-1} can be assigned to the modes 10 and 11 in A and B. The former mode has the predominant contribution from the in-plane δ(N3H) vibration, while the latter is due to a stretching vibration of the uracil ring (Table 4).

According to the calculated PED, the δ(OH) bending in the carboxylic group is strongly coupled with the ν(C7—O9) stretching vibration. For A, these mixed vibrations give rise to two normal modes, 12 and 15, with the anharmonic frequencies 1346 cm^{-1}

and 1134 cm^{-1}, respectively (see Table 4). In the experimental spectrum of orotic acid in Ar matrix, the corresponding bands are observed at 1354 cm^{-1} and 1166 cm^{-1} (Fig. 4). For comparison, in the IR spectrum of benzoic acid in solid Ar [39], the analogous bands were found at 1347 and 1169 cm^{-1}. The similar frequencies of the corresponding normal modes of orotic and benzoic acids, support the assignments proposed in Table 5.

However, it should be noted that the B3LYP-predicted anharmonic frequencies of the modes 10, 11 and 15 (mainly due to δ(N3H) bending, ring stretching, and δ(OH) bending vibrations, respectively) are underestimated by about 20–30 cm^{-1}, relative to the experiment.

Comparison of the experimental and theoretical spectra of orotic acid, in the range 800–400 cm^{-1}, is illustrated in Fig. 5. Two strong bands at 781 and 758 cm^{-1} appear in the experimental spectrum. These bands can be reliably assigned, because the 800–750 cm^{-1} region of the spectrum is very well reproduced by the theoretical calculations. The normal mode of A (21A) assigned to the band at 781 cm^{-1} has the predominant contribution from the out-of-plane
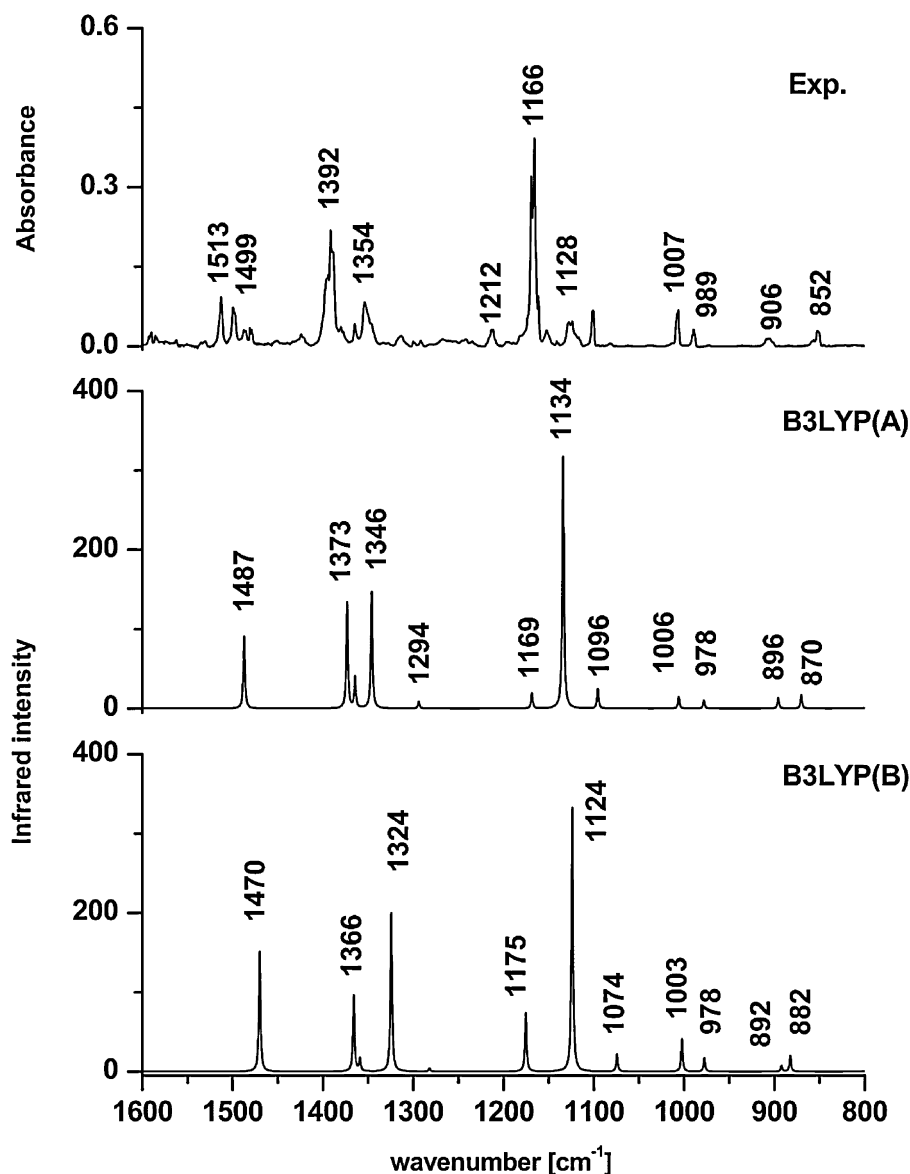
Fig. 4. Comparison of the experimental IR spectra of orotic acid isolated in an argon matrix with the theoretical spectra calculated for conformers A and B at the B3LYP/aug-cc-pVTZ level (region 1600–800 cm^{-1}). The theoretical wavenumbers were calculated using the anharmonic approach and the IR intensities were calculated within the harmonic approximation.

vibration of the carboxylic COO group (74%) mixed with the out-of-plane γ(C4=O) bending vibration (Table 4). A similar mode in B (21B) may also be assigned to this experimental band. The other strong band, at 758 cm^{-1}, is due to the out-of-plane γ(C2=O) vibration (78%) coupled with the out-of-plane γ(N3H) vibration (mode 22 in A and B). The anharmonic frequencies (789 and 763 cm^{-1}, calculated for conformer A) are in very good agreement with the spectral position of the two experimental IR bands discussed above.

For comparison, in the IR spectrum of uracil in an Ar matrix, the band assigned to the γ(C2=O) vibration was observed at 757 cm^{-1} [40,41]. This frequency is nearly identical with the spectral position (758 cm^{-1}) of the γ(C2=O) band in the spectrum of orotic acid.

The band due to the out-of-plane γN3H vibration in orotic acid was observed at 662 cm^{-1}. This is also in excellent agreement with the assignment reported for uracil in solid Ar, where the corresponding band was found at the same frequency, 662 cm^{-1} [40,41].

The broad split band at 578/572 cm^{-1} has been assigned to the OH torsional vibration. The predicted anharmonic frequency of this mode (594 cm^{-1} for conformer A) is somewhat overestimated. The assignments of the remaining bands in the spectrum of matrix-isolated orotic acid are shown in Table 5.

5. Experimental estimation of the mole fraction of conformers from the IR spectra versus theoretical predictions

Due to significant overlap of the absorption bands of two conformers (A and B), occurring throughout nearly the whole IR spectrum, the estimation of the relative populations of the two forms trapped in solid Ar is not a straightforward task. The best set of data facilitating such an assessment is provided by the bands due to the stretching vibrations of the OH and NH bonds. In this respect, the experimental intensities of the bands assigned to the modes 1A, 1B and 2B (see Tables 4 and 5) can be used for the most
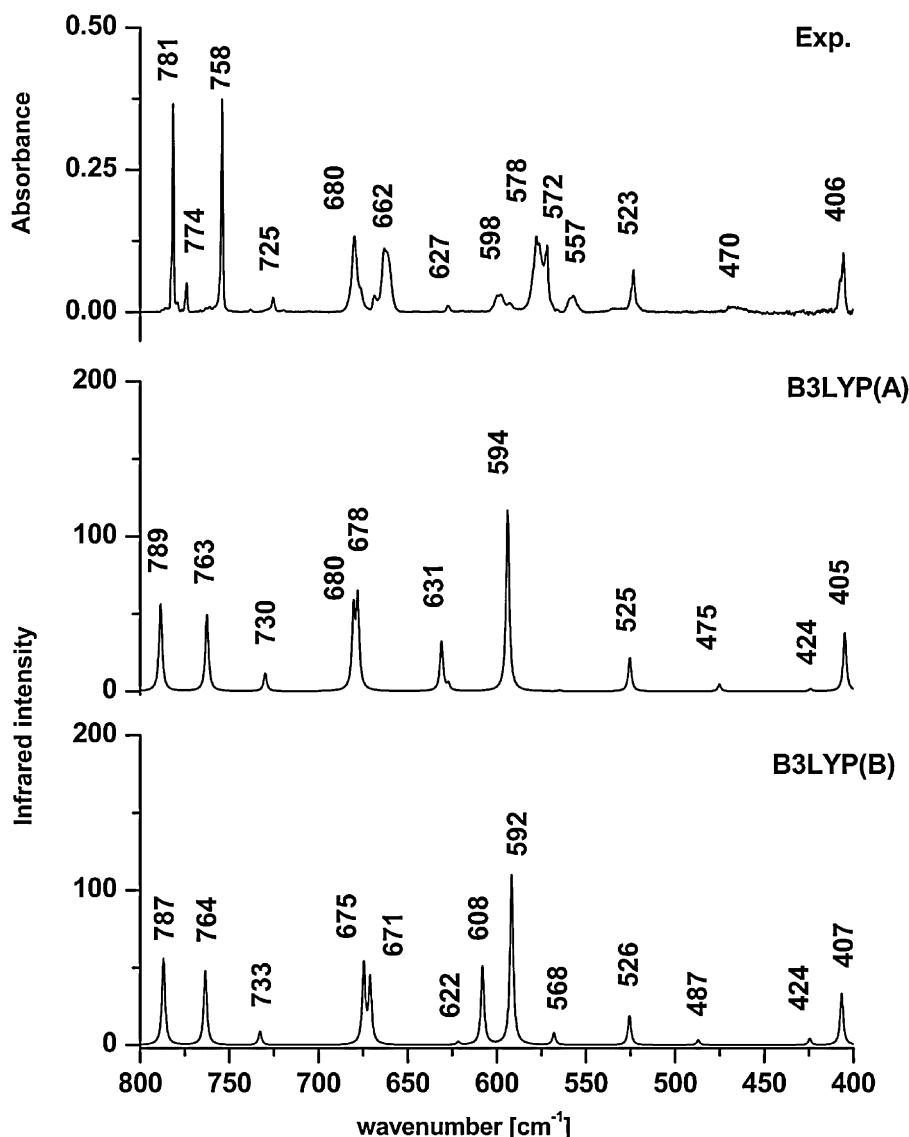
Fig. 5. Comparison of the experimental IR spectra of orotic acid isolated in an argon matrix with the theoretical spectra calculated for conformers A and B at the B3LYP/aug-cc-pVTZ level (region 800–400 cm^{-1}). The theoretical wavenumbers were calculated using the anharmonic approach and the IR intensities were calculated within the harmonic approximation.

reliable estimation. The mole fraction existing in the matrix can be assessed by taking into account the experimental intensities of the bands observed at 3563 and 3460 cm^{-1} (Table 5) as well as theoretical absolute intensities of modes 1A, 1B and 2B (Table 4). Assuming that the calculated IR intensities of the normal modes 1A, 1B, and 2B are reliable, the formula for the intensity ratio can be written as follows:

$$\frac{I_{3563}}{I_{3460}} = \frac{A_{1A} \times n_A + A_{1B} \times n_B}{A_{2B} \times n_B}, \tag{1}$$

where n_A and n_B are the populations of A and B, respectively; I_{3563} and I_{3460} are the integrated intensities of the experimental bands at 3563 and 3460 cm^{-1}, respectively, and A_{1A}, A_{1B}, and A_{2B} are the theoretical absolute intensities of modes 1A, 1B and 2B.

From the above relation one obtains the formula for the population ratio:

$$\frac{n_A}{n_B} = \frac{I_{3563}}{I_{3460}} \times \frac{A_{2B}}{A_{1A}} - \frac{A_{1B}}{A_{1A}}. \tag{2}$$

Using the data from Tables 4 and 5, one can estimate the n_A/n_B ratio as equal to 5.6. In other words, the mole fraction of the orotic acid molecules adopting the B form can be assessed as ca. 15%.

This result and the fact that there are no spectral indications of the presence of isomers C and D in solid argon are in line with the recently reported study of the E/Z conformational isomerization of benzoic acid using matrix isolation techniques [20]. Schreiner at coworkers have demonstrated that the higher lying E conformer of benzoic acid could not be observed in an argon matrix because of fast H-tunneling to the more stable conformer Z (a half-life time is only about 10^{-5} min in Ar at 11 K) [20]. By analogy to benzoic acid, a similar effect should also occur in our experimental study. Thus, if the C and D isomers of orotic acid are present in the gas phase (these isomers correspond to the E conformer of benzoic acid) they should convert quickly back to the A and B conformers, respectively, in matrix. For example, the total population of isomer A in an argon matrix should be equal to the sum of the populations of A and C, calculated for the gas phase. Thus, according to the B3LYP results, the expected populations of A and B in solid matrix should be about 82.4% (76.8 + 5.6) and

Table 5
Experimental wavenumbers (ν, cm^{-1}) and integrated relative intensities (I) of the absorption bands observed in the IR spectrum of orotic acid monomers isolated in an argon matrix.

Ar matrix		Assignment mode no.[a]	Approximate mode description[a]
ν	I		
3563	187	1A + 1B	νOH
3460	28	2B	νN1H
3428	280	2A + 3A + 3B	νN3H, νN1H
1785		1392 + 406	
1780	49	5B	νC7=O8
1765	705	5A + 6A + 6B	νC2=O + νC7=O8
1761			
1734		1212 + 523	
1721	901	7A + 7B	νC4=O
1704		Overtone (2·852)	
1645	28	8A + 8B	νC5=C6
1513		Overtone (2·758)	
1499	108	9A + 9B	νU$_{ring}$, δN1H
1395	181	10A + 11A + 10B + 11B	δN3H, νU$_{ring}$, δN1H
1392			
1354	71	12A	δOH, νC7O9
1314	13	12B	νU$_{ring}$, δOH, νC7O9
1212	29	14A + 14B	νU$_{ring}$
1170	267	15A + 15B	δOH, νC7O9
1166			
1128		Overtone (2·557)	
1101	21	16A	νU$_{ring}$
1081	2	16B	νU$_{ring}$
1007	27	17A + 17B	δU$_{ring}$
989	11	18A + 18B	δU$_{ring}$
906	20	19A + 19B	νU$_{ring}$
857	5	20B	γC5H
852	11	20A	γC5H
781	41	21A + 21B	γCOO
774			
758	48	22A + 22B	γC2=O
725	5	23A + 23B	γC4=O
680	53	24A + 24B	δ_{sc}COO
662	65	25A + 25B	γN3H
598	17	27A	γN1H
593	3	27B	τOH
578	86	28A	τOH
572			
557	14	28B	γN1H
523	22	30A + 30B	δU$_{ring}$
470		31A + 31B	γCOO
406	32	33A + 33B	δU$_{ring}$, δC4=O

[a] For details, see Table 4.

17.6%, respectively. These values are in a good agreement with the experimental findings.

6. Conclusions

Orotic acid (6-carboxyuracil, also called vitamin B$_{13}$) plays a fundamental role in the biosynthesis of all pyrimidine bases in DNA and RNA. Thus, a full understanding of the vibrational spectra of this compound is of great importance. In this work, the FT-IR spectrum of orotic acid monomers isolated in a low temperature argon matrix is reported for the first time. Rotational isomerism is an intriguing feature of carboxylic acids, and this phenomenon has also been investigated in this work. The main results can be summarized as follows:

(1) All the theoretical methods (ab initio MP2 and three density functional methods, B3LYP, M06 and M06-2X) consistently predict that four possible conformers of orotic acid A, B, C and D may exist in the gas phase. The A and B conformers differ by the relative position of the carboxyl C=O group with respect to the C=C bond of the uracil ring, while C and D isomers arise from the rotation of the carboxylic O—H bond around the C—O bond in A and B, respectively (see Fig. 1). Only structures A and B are planar, isomer C is slightly distorted from planarity, while in isomer D the carboxyl group is tilted by about 30–32° out of the plane of the uracil ring.

(2) In the recently reported work [25] it has been shown that out of 27 various DFT methods, M06-2X is the best for predicting the barrier heights. Therefore, we consider that the results from calculations of the rotational barrier performed at the M06-2X/aug-cc-pVTZ level, are fairly accurate. The predicted rotational barrier heights for the conversions A → B, A → C and B → D are 37.1, 47.5 and 51.3 kJ mol^{-1}, respectively.

(3) A reliable estimation of the relative stability and the mole percentages of all isomers of orotic acid in the gas phase have been obtained from the Gibbs free energies (ΔG°_{T}) calculated for 480 K (the temperature of evaporation of orotic acid).

(4) The anharmonic vibrational frequencies have been computed at the B3LYP/aug-cc-pVTZ level. The spectrum calculated for conformer A matches very well the experimental spectrum. Some bands due to conformer B have also been identified. No spectral indications of the presence of the other isomers, C and D, in the matrix were detected.

(5) From the experimental data (the measured experimental intensities of the bands due to the ν(O—H) and ν(N—H) stretching vibrations of the two stable conformers) and the computed absolute intensities of the corresponding modes, the population of A and B conformers of orotic acid in a low temperature Ar matrix has been calculated. The mole fraction of the less stable B form is ca. 15%, which is in good agreement with the DFT results.

Appendix A. Supplementary data

Supplementary data associated with this article can be found, in the online version, at http://dx.doi.org/10.1016/j.vibspec.2012.11.002.

References

[1] A. Lehninger, Principles of Biochemistry, Worth Publishers, New York, 1970, p. 661.
[2] J. Victor, L.B. Greenberg, D.L. Sloan, J. Biol. Chem. 254 (1979) 2647.
[3] M. Falk, Pharmazie 40 (1985) 377.
[4] H. Van der Meersch, J. Pharm. Belg. 4 (2006) 97.
[5] H. Schmidbaur, H.G. Classen, J. Helbig, Angew. Chem. 102 (1990) 1122.
[6] O. Kumberger, J. Riede, H. Schmidbaur, Z. Naturforsch. B 48 (1993) 961.
[7] P. Castan, E. Colacio-Rodriguez, A.L. Beauchamp, S. Cros, S. Wimmer, J. Inorg. Biochem. 38 (1990) 225.
[8] F.L. Rosenfeldt, Cardiovasc. Drugs Ther. 12 (1998) 147.
[9] H. Jellinek, E. Takacs, Arzneimittelforschung 50 (2000) 1071.
[10] O.K. Yesilel, M.S. Soylu, H. Ölmez, O. Büyükgüngör, Polyhedron 25 (2006) 2985, and references therein.
[11] R. Wysokiński, B. Morzyk-Ociepa, T. Głowiak, D. Michalska, J. Mol. Struct. 606 (2002) 241.
[12] R. Wysokiński, K. Hernik, R. Szostak, D. Michalska, Chem. Phys. 333 (2007) 37.
[13] D. Michalska, K. Hernik, R. Wysokiński, B. Morzyk-Ociepa, A. Pietraszko, Polyhedron 26 (2007) 4303.
[14] K. Helios, R. Wysokiński, W. Zierkiewicz, L.M. Proniewicz, D. Michalska, J. Phys. Chem. B 113 (2009) 8158.
[15] K. Helios, A. Pietraszko, R. Wysokiński, D.P. Strommen, D. Michalska, Vib. Spectrosc. 52 (2010) 1.

[16] K. Helios, R. Wysokiński, A. Pietraszko, D. Michalska, Vib. Spectrosc. 55 (2011) 207.
[17] F. Takusagawa, A. Shimada, Bull. Chem. Soc. Jpn. 46 (1973) 2011.
[18] G. Portalone, Acta Crystallographica E 64 (2008) o656.
[19] A. Hernanz, F. Billes, I. Bratu, R. Navarro, Biopolymers (Biospectrosc.) 57 (2000) 187.
[20] S. Amiri, H.P. Reisenauer, P.R. Schreiner, J. Am. Chem. Soc 132 (2010) 1592, and references therein.
[21] H. Rostkowska, L. Lapinski, M.J. Nowak, Vib. Spectrosc. 49 (2009) 43.
[22] A.D. Becke, J. Chem. Phys. 104 (1996) 1040.
[23] C. Lee, W. Yang, R.G. Parr, Phys. Rev. B 37 (1988) 785.
[24] Y. Zhao, D.G. Truhlar, Theor. Chem. Acc. 120 (2008) 215.
[25] A.J. Cohen, P. Mori-Sánchez, W. Yang, Chem. Rev. 112 (2012) 289.
[26] T.H. Dunning Jr., J. Chem. Phys. 90 (1989) 1007.
[27] R.A. Kendall, T.H. Dunning, R.J. Harrison Jr., J. Chem. Phys. 96 (1992) 6796.
[28] C. Møller, M.S. Plesset, Phys. Rev. 46 (1934) 618.
[29] T.H. Dunning, P.J. Hay, in: H.F. Schaefer III (Ed.), Modern Theoretical Chemistry, vol. 4, Plenum Press, New York, 1977.
[30] C. Peng, P.Y. Ayala, H.B. Schlegel, M.J. Frisch, J. Comput. Chem. 17 (1996) 49.
[31] C. Peng, H.B. Schlegel, Israel J. Chem. 33 (1993) 449.
[32] V. Barone, J. Chem. Phys. 120 (2004) 3059.
[33] V. Barone, J. Chem. Phys. 122 (2005) 014108.
[34] M.J. Frisch, G.W. Trucks, H.B. Schlegel, G.E. Scuseria, M.A. Robb, J.R. Cheeseman, G. Scalmani, V. Barone, B. Mennucci, G.A. Petersson, H. Nakatsuji, M. Caricato, X. Li, H.P. Hratchian, A.F. Izmaylov, J. Bloino, G. Zheng, J.L. Sonnenberg, M. Hada, M. Ehara, K. Toyota, R. Fukuda, J. Hasegawa, M. Ishida, T. Nakajima, Y. Honda, O. Kitao, H. Nakai, T. Vreven, J.A. Montgomery Jr., J.E. Peralta, F. Ogliaro, M. Bearpark, J.J. Heyd, E. Brothers, K.N. Kudin, V.N. Staroverov, R. Kobayashi, J. Normand, K. Raghavachari, A. Rendell, J.C. Burant, S.S. Iyengar, J. Tomasi, M. Cossi, N. Rega, J.M. Millam, M. Klene, J.E. Knox, J.B. Cross, V. Bakken, C. Adamo, J. Jaramillo, R. Gomperts, R.E. Stratmann, O. Yazyev, A.J. Austin, R. Cammi, C. Pomelli, J.W. Ochterski, R.L. Martin, K. Morokuma, V.G. Zakrzewski, G.A. Voth, P. Salvador, J.J. Dannenberg, S. Dapprich, A.D. Daniels, O. Farkas, J.B. Foresman, J.V. Ortiz, J. Cioslowski, D.J. Fox, Gaussian 09, Revision A.02, Gaussian, Inc., Wallingford, CT, 2009.
[35] D.C. Bieńko, D. Michalska, S. Roszak, W. Wojciechowski, M.J. Nowak, L. Lapinski, J. Phys. Chem. A 101 (1997) 7834.
[36] M.J. Nowak, L. Lapiński, D.C. Bieńko, D. Michalska, Spectrochim. Acta 53A (1997) 855.
[37] K. Aarset, E.M. Page, D.A. Rice, J. Phys. Chem. A 110 (2006) 9014.
[38] G. Bazsó, G. Tarczay, G. Fogarasi, P.G. Szalay, Phys. Chem. Chem. Phys. 13 (2011) 6799.
[39] S.G. Stepanian, I.D. Reva, E.D. Radchenko, G.G. Sheina, Vib. Spectrosc. 11 (1996) 123.
[40] A.J. Barnes, M.A. Stuckey, L. Le Gall, Spectrochim. Acta 40A (1984) 419.
[41] A. Leś, L. Adamowicz, M.J. Nowak, L. Lapinski, Spectrochim. Acta 48A (1992) 1385.
[42] M. Graindourze, J. Smets, Th. Zeegers-Huyskens, G. Maes, J. Mol. Struct. 222 (1990) 345.
[43] G.N. Ten, V.V. Nechaev, S.V. Krasnoshchekov, Optics Spectrosc. 108 (1) (2010) 37–44.
[44] W.B. Person, K. Szczepaniak, Calculated and experimental vibrational spectra and force fields for isolated pyrimidine bases, in: J.R. Durig (Ed.), Vibrational Spectra and Structure, vol. 20, Elsevier, Amsterdam, 1993, p. 239.
[45] B. Morzyk-Ociepa, M.J. Nowak, D. Michalska, Spectrochim. Acta A 60 (2004) 2113.
[46] L. Lapinski, M.J. Nowak, D.C. Bieńko, D. Michalska, Phys. Chem. Chem. Phys. 4 (2002) 1123.